I&EC research
Industrial & Engineering Chemistry Research

pubs.acs.org/IECR

Article

# Environmental Aging of Polymers to Evaluate Their Potential for Remediating Natural Gas Pipelines

Mohammadjavad Haji Rezaei, Aiden Ferreira, Maile Campbell, Deepro Ghosh, Keven Alkhoury, Zakhar Lyakhovych, Edith Mathiowitz, Vikas Srivastava, and Ryan Poling-Skutvik*

Cite This: https://doi.org/10.1021/acs.iecr.5c02255



**ABSTRACT:** We assess the aging of polymeric materials in natural gas environments for potential applications in pipeline remediation as liner materials. Three commercially available polymers—high-density polyethylene (HDPE), Nylon-6/6 polyamide (PA), and polyvinylidene fluoride (PVDF)—are aged under accelerated conditions in a model natural gas environment of pure alkanes at 250 PSI and 90 °C for up to 30 days. The Young's modulus and yield stress of these polymers remain unchanged within experimental error after exposure to the natural gas environment. Dynamic mechanical analysis, however, reveals drastic changes to polymer chain dynamics, with the activation energy for segmental relaxations reduced by up to 50%, corresponding to accelerated molecular motion. The environmental aging is confirmed through FTIR, which found an increase in the density of natural gas molecules within the polymer matrices. Additionally, these changes in the dynamics within polymeric solids are reversible; prolonged removal from the gas atmosphere resulted in the activation energies returning to near-initial values within 2 weeks. These observations suggest that this aging response is dominated by physical processes in which the polymers absorb natural gas molecules due to the increase in partial pressures, as opposed to a chemical mechanism in which the natural gas reacts irreversibly with the polymer chains. In applications for pipeline remediation, our results indicate that polymeric liners will provide sufficient mechanical rigidity but may suffer from accelerated rates of creep facilitated by the increase in local polymer dynamics.

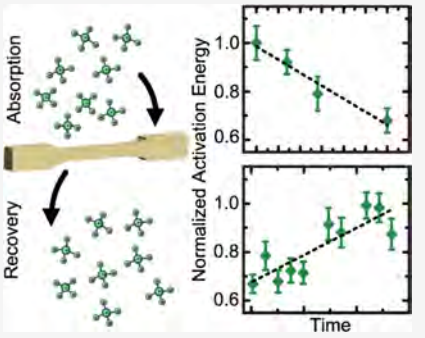




## 1. INTRODUCTION

The United States natural gas distribution system is an essential component of the nation's energy infrastructure, consisting of approximately 2.3 million miles of pipelines that distribute natural gas to residential and commercial consumers.[1,2] Major portions of these pipelines consist of cast iron, which has been in use in the oil and gas industry for many decades, especially within the New England region.[2,3] Some of these cast iron pipelines have been in operation for decades, making them increasingly susceptible to deterioration due to prolonged exposure to environmental conditions.[4−6] In addition to external environmental effects, internal corrosion of natural gas pipelines can be caused by the presence of impurities such as carbon dioxide ($CO_2$), hydrogen sulfide ($H_2S$), and water, as well as microbial activities.[7] Among the various forms of corrosion, $CO_2$-induced (sweet corrosion) and $H_2S$-induced (sour corrosion) are the most common, influenced by the gas composition, moisture content, flow regime, and the surface characteristics of pipeline materials.[4,5] These combined effects can result in leaks that result in an economic burden often passed on to consumers and that pose a significant risk to environmental and community safety.

Historically, installation, rehabilitation, and construction of buried pipes have been based on the use of the open-cut pipeline installation (OCPI) process, which entails digging a trench to replace buried pipes. OCPI is time-consuming and labor intensive, and in most cases, leads to extensive disturbance, especially in urban environments.[8] The presence of existing infrastructure such as water pipes, electrical wiring, and other underground services further complicates the practice. Additionally, excavation risks soil subsidence and collapse, compromising structures and damaging the environment. In some cases, geographical constraints or other physical obstacles render direct excavation impossible, necessitating alternative methods of pipeline installation and maintenance.[9−12]

To avoid challenges and reduce costs associated with OCPI, alternative methods of remediation have been considered, most commonly using polymeric materials.[5,7,13−17] Polymers are promising candidates for the rehabilitation of cast iron pipes due to their low cost and ease of processing as well as their high corrosion resistance and favorable strength-to-weight ratio.[5] Trenchless pipeline rehabilitation methods most

Received: June 3, 2025
Revised: August 5, 2025
Accepted: August 19, 2025

commonly use sliplining or cured-in-place pipe (CIPP) approaches, both of which have different benefits for rehabilitating aging infrastructure without major excavation. In sliplining, a carrier pipe of smaller diameter is inserted into an existing host pipeline, frequently grouted into position to provide additional structural support. Even with the decreased interior diameter, the increased smoothness of the replacement pipe normally retains or even improves flow efficiency. CIPP utilizes a flexible liner that is expanded and cured within the old pipeline by either heat or light to create a jointless, seam-free pipe. Not only does this approach restore structural integrity but easily handles bends and a wide variety of pipeline geometries.[18−21] In either approach, the polymer liners must be mechanically rigid to provide structural strength throughout their lifespan. Furthermore, they must resist the unique conditions of natural gas environments, including potential chemical interactions, pressure changes, and thermal fluctuations. Therefore, it is essential to understand any effect that natural gas environments may have on the chemical, mechanical, and dynamical properties of polymers to ensure safe and effective operation as pipeline remediation agents.

Many researchers have previously studied the mechanism of gas-induced plasticization in polymeric solids.[22−26] Gas molecules may work as a molecular lubricant enhancing chain mobility,[22] they can form specific interactions with polar groups promoting physical transitions,[23] or they can induce polymer swelling to increase in the free volume.[24] Often, this plasticization effect is identified through changes in molecular permeability, whereby an increase in gas transport is correlated with increased plasticization. The resulting impact of such gas absorption on the mechanical properties of these polymers is more difficult to determine due to the relatively small changes occurring in the bulk. There remains an open question as to how to identify subtle changes in mechanics that could lead to new mechanisms underlying mechanical failure.

In this work, we expose and age a variety of industrial polymers to a model gas environment and measure the effect on their mechanical and dynamical properties. Through linear dynamic mechanical analysis (DMA) and quasistatic tensile tests, we find that the elastic and yield properties of the polymers remain unchanged during exposure to natural gas environments. By contrast, we observe significant changes to the relaxation behavior and viscoelastic response of the polymers, as quantified through the shift factors underlying time−temperature superposition. Our results reveal a reversible decrease in the activation energy controlling segmental relaxations following gas exposure, indicating that the gas molecules act as plasticizers to enhance dynamic fluctuations. When removed from the natural gas environments, the polymers recover toward their original relaxation spectra. This recovery suggests that the plasticization occurs through physical absorption, which is confirmed through Fourier transform infrared spectroscopy. Our findings provide important insight into the time-dependent behavior and durability of polymeric liners under realistic natural gas service conditions and demonstrate that polymers can effectively serve to remediate natural gas pipelines.

## 2. METHODS AND MATERIALS

**2.1. Sample Preparation.** Commercially available sheets of high-density polyethylene (HDPE), Nylon-6/6 polyamide (PA), and polyvinylidene fluoride (PVDF) were purchased from McMaster. HDPE and PA sheets had a nominal thickness of 3.18 mm while PVDF sheets had a nominal thickness of 6.36 mm. Dog-bone specimens were machined using a Mill Computer Numerical Control (CNC) machine according to ASTM D638-V. For HDPE and PA, samples were directly cut from the purchased sheets. For PVDF, smaller strips measuring 80 mm × 15 mm were extracted and then further machined. The nominal gauge section dimensions for all samples are 9.53 mm long, 3.18 mm wide, and 3.18 mm thick. All samples were measured before testing due to the expected small variability from dimensional tolerance. In addition, rectangular samples measuring 12.7 mm in length by 3.2 mm in thickness were fabricated for dynamic mechanical analysis following the ASTM D790−17 standard.

**2.2. Dynamic Mechanical Analysis.** Dynamic mechanical analysis (DMA) in 3-point bending mode was conducted on a TA Instruments HR-20 rheometer to characterize the viscoelastic moduli of the materials across a range of frequencies. A preload force of 5 ± 0.1 N was applied before initiating the frequency sweep at each temperature to ensure sufficient contact between the instrument and the sample. An axial displacement of 7 $\mu$m was maintained during the measurements. The frequency sweep was performed over a range of $f$ = 0.005 to 1 Hz at temperatures ranging from 25 °C to 105 °C in increments of 10 °C. Samples were allowed to equilibrate for 10 min after each temperature change to ensure uniform temperature within the sample.

**2.3. Uniaxial Experimental Setup.** Uniaxial tensile tests were performed using an MTS Bionix Servohydraulic testing machine. A 25 kN load cell (MTS Model 662.20H-05) was used to measure the force, which was then converted to the nominal stress. The Digital Image Correlation (DIC) software MatchID 2D, integrated with a FLIR Blackfly S USB3 camera, was used to measure the nominal strain $\varepsilon$ during the experiments. Uniaxial tension tests were conducted at room temperature and the nominal stress $\sigma$ was measured as a function of $\varepsilon$ at a nominal strain rate of $\dot{\varepsilon} = 2 \times 10^{-4}$ s$^{-1}$ until the point of necking. From these measurements, the Young's modulus $E$ was calculated from the initial linear slope to 1% strain, and the yield stress $\sigma_y$ was determined using the 0.2% offset method.

**2.4. Fourier Transform Infrared Spectroscopy.** The chemical structure of the samples was analyzed by Attenuated Total Reflectance Fourier Transform Infrared (ATR-FTIR) spectroscopy using a PerkinElmer Spectrum 2 spectrophotometer scanning over wavelengths ranging from 4000 to 500 cm$^{-1}$ with a resolution of 4 cm$^{-1}$ for a total of 10 scans per sample. To assess changes in polymer composition with gas exposure, the spectra were normalized to characteristic peaks with Spectragryph, a postspectral processing software. At least three samples were measured for each polymer aging condition to assess variability and error.

**2.5. Aging Protocol.** Samples were placed inside a pressure vessel using a custom-made holder to hold the samples in an upright position and ensure good contact with the gaseous environment. The vessel was evacuated under vacuum to remove air, after which it was filled with a natural gas mixture purchased from Airgas consisting of 80% methane, 10% ethane, 7% propane and 3% $n$-butane. The aging process was conducted at a temperature of 90 °C and a pressure of 250 PSI (≈1700 kPa) for durations up to 30 days. This elevated temperature was chosen to account for possible chemical changes occurring in these polymers. Assuming an activation energy of 100 kJ/mol, an order of magnitude common for


https://doi.org/10.1021/acs.iecr.5c02255
Ind. Eng. Chem. Res. XXXX, XXX, XXX−XXX

many chemical reactions, this elevated temperature results in a dramatic enhancement of the effective aging time. Mathematically, the ratio of effective aging times can be calculated according to

$$\frac{t}{t_{ref}} = \exp\left[-\frac{E_a}{R}\left(\frac{1}{T} - \frac{1}{T_{ref}}\right)\right] \quad (1)$$

One month of aging at $T$ = 90 °C would therefore correspond to approximately 100 years of aging at $T_{ref}$ = 25 °C. Another set of samples was also aged for 30 days at room temperature for comparison.

## 3. RESULTS AND DISCUSSION

**3.1. Solid Mechanics.** The mechanical properties of the neat polymer samples at $T$ = 25 °C are measured as a function of frequency $f$ using DMA, as shown in Figure 1. The three

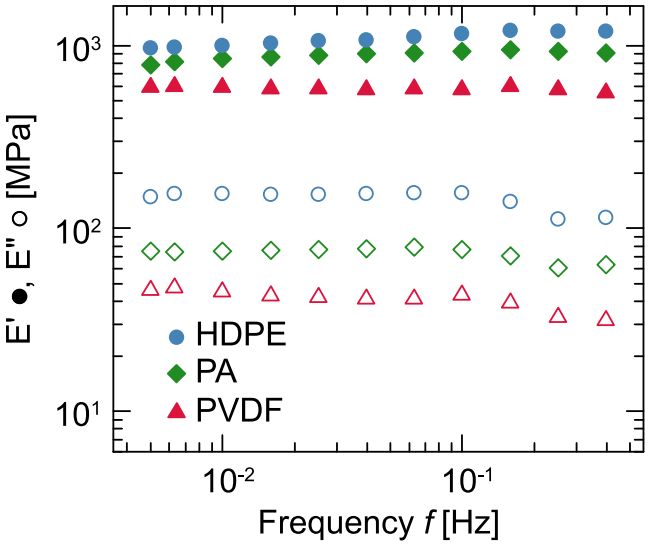


**Figure 1.** Storage modulus $E'$ (closed) and loss modulus $E''$ (open) at $T$ = 25 °C as a function of frequency $f$ for HDPE, PA and PVDF.

polymer chemistries—high density polyethylene (HDPE), Nylon-6/6 polyamide (PA), and poly(vinyl difluoride) (PVDF)—exhibit similar relaxation spectra and moduli, sufficient to provide mechanical rigidity as pipeline liners. Specifically, we observe that the storage (elastic) modulus $E'$ of these materials ranges between 500 MPa and 2 GPa and are weak functions of frequency $f$. These measurements are consistent with a wide body of literature results on the viscoelasticity of neat polymer solids,[27−33] and serve as the benchmark against which we will evaluate the impact of natural gas exposure.

Following linear DMA, the polymers samples are incubated in pressure chambers in a model natural gas environment consisting of 80% methane, 10% ethane, 7% *n*-propane, and the balance *n*-butane at a pressure of 250 PSI and a temperature of 90 °C for up to 30 days. This pressure is chosen to approximate the general operating conditions in transmission pipelines and an upper maximum on the operating pressures for distribution pipelines,[2,34] which are the primary candidate for remediation. The elevated temperature would accelerate the aging process for chemical effects, which can be assessed by comparing the mechanical response of polymers aged under high temperature to those aged at room temperature conditions.

The mechanical properties of the aged polymer samples are measured within 48 h after removal from the natural gas environment to minimize potential changes that could occur under atmospheric conditions. We find that the Young's modulus $E$ does not significantly change after exposure to the natural gas environment (Figure 2(a−c)). These measurements are confirmed through both DMA and tensile measurements across all three polymer chemistries. We do note, however, that there are significant fluctuations in the measured data which may overwhelm any detectable signal. Nevertheless, these fluctuations demonstrate that the mechanical modulus may not be a sensitive metric of aging in natural gas environments. Additionally, the polymer deformation mechanics appear to be independent of the aging temperature. The moduli measured after 30 days of exposure at 90 °C and at room-temperature (i.e., 20−25 °C) have comparable moduli within experimental error. This temperature independence suggests that there is no significant degradation in the material, which would be accelerated through Arrhenius-like processes at elevated temperatures.

The Young's modulus characterizes the linear response of these materials to small deformations, but high loads leading to plastic/nonlinear response causing loss of material stiffness can lead to mechanical failure. The yield stress $\sigma_y$ is one characteristic property that represents the onset of plasticity defined under tensile deformation as the stress beyond which the stress−strain relation of the material deviates from a linear elastic response. Similar to our observations for the modulus, we do not observe any significant or reproducible effect of aging in the presence of natural gas on the yield stress of these polymer solids across the various polymer chemistries (Figure 2d−f). Again, samples aged under elevated and room temperature conditions exhibit comparable properties. Together, these findings demonstrate that the linear elastic and nonlinear plastic mechanical deformation responses of neat polymer solids measured at room temperature are preserved after being exposed to natural gas.

**3.2. Viscoelastic Shifts.** Polymers are inherently viscoelastic. Thus, even despite the lack of any detectable effect of natural gas on Young's modulus $E$ and the yield stress $\sigma_y$, there may still be changes to the viscoelastic relaxations of these materials. To probe these effects, we conduct DMA measurements at various temperatures in which we subject the material to an oscillatory strain with an amplitude within the linear viscoelastic regime (Figure 3a). As $T$ increases, the viscoelastic moduli decrease and exhibit a slightly stronger frequency dependence. We exploit time−temperature superposition (TTS) to construct a master curve for each polymer by shifting the frequency by a temperature-dependent shift factor $a_T$ until it overlaps with the reference spectrum at $T$ = 25 °C (Figure 3b).[35−40] The shifted frequency collapses both the storage modulus $E'$ and the loss modulus $E''$ onto a single master curve that quantifies the relaxations of the polymers over many decades of frequency. We observe a broad relaxation in these solids with $E'$ increasing by an order of magnitude over shifted frequency regime. For all measured frequencies (and temperatures), the polymers behave as viscoelastic solids with $E' > E''$ as expected for temperatures below the melting point.

The shift factor $a_T$ is typically associated with the activation of dynamic relaxations within the polymer chain. We find that


https://doi.org/10.1021/acs.iecr.5c02255
Ind. Eng. Chem. Res. XXXX, XXX, XXX−XXX

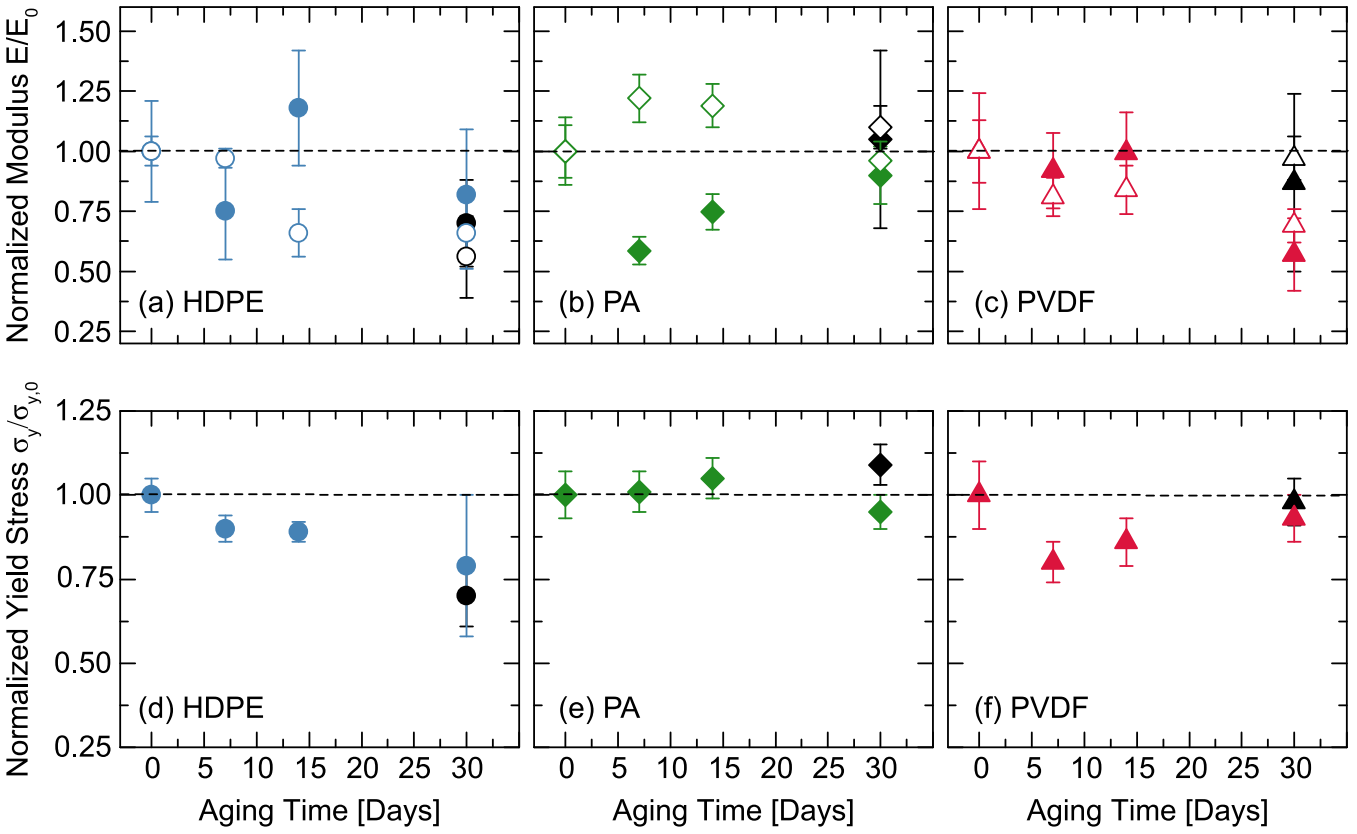


**Figure 2.** Normalized Young's modulus $E/E_0$ determined from DMA (solid) and tensile tests (open) conducted at 25 °C and normalized yield stress $\sigma_y/\sigma_{y,0}$ as a function of aging time at 90 °C for (a) and (d) HDPE, (b) and (e) PA, (c) and (f) PVDF. Black symbols represent measurements taken after aging at room temperature.

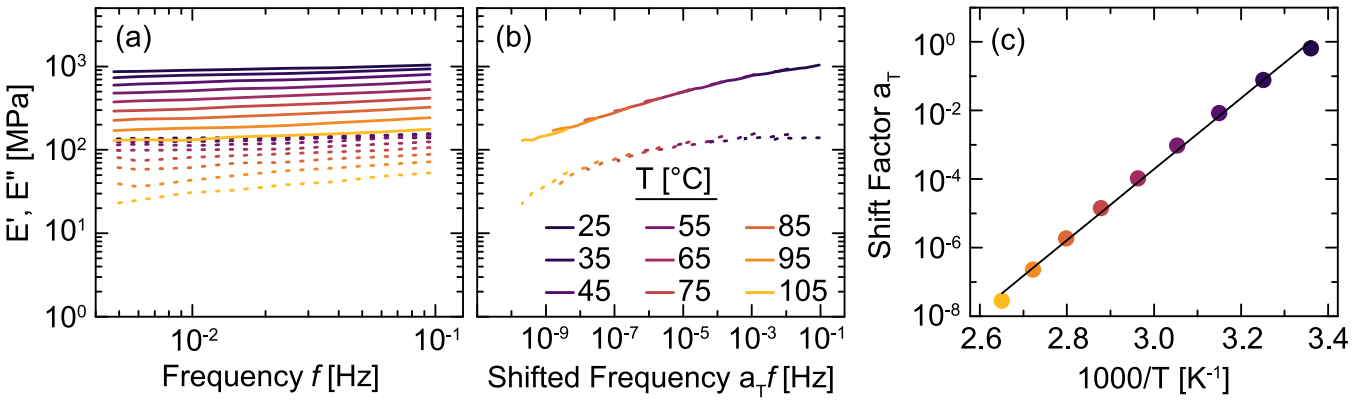


**Figure 3.** (a) Storage $E'$ (solid line) and loss $E''$ (dash line) moduli as a function of frequency $f$ for HDPE. (b) HDPE master curve obtained by TTS with shift factors $a_T$. (c) Shift factors $a_T$ for HDPE as a function of inverse temperature $T^{-1}$. Solid line is fit to eq 2.

$a_T$ follows an Arrhenius dependence on temperature according to

$$a_T = \exp\left(\frac{-E_a}{RT}\right) \tag{2}$$

where $E_a$ is the activation energy for the relaxation process, $R$ is the ideal gas constant, and $T$ is the absolute temperature,[35,41] as shown in Figure 3c. This Arrhenius behavior is expected for polymers well above their glass transition temperature $T_g$.[42] From this fit, we extract the activation energy for the neat polymer solids $E_{a,0}$ = 200 ± 7, 312 ± 16, and 289 ± 50 kJ/mol for HDPE, PA, and PVDF, respectively. These measurements are consistent with previously reported values for HDPE,[43] PA,[44] and PVDF[45] over comparable temperature ranges.

The temperature dependent shift factors $a_T$ quantify changes to polymer segmental dynamics, allowing us to investigate how dynamic relaxations depend on natural gas exposure. We observe a continuous decrease in the slope of these Arrhenius plots with increasing exposure time across all polymer chemistries, indicating a significant reduction in their activation energy $E_a$, as shown in Figure 4. This decrease in $E_a$ suggests that exposure of polymers to natural gas leads to an increase in the rate at which the polymer chains relax. The effect is slightly different across the three polymers, with HDPE showing the most pronounced reduction in $E_a$, followed by PA, while PVDF


https://doi.org/10.1021/acs.iecr.5c02255
Ind. Eng. Chem. Res. XXXX, XXX, XXX−XXX

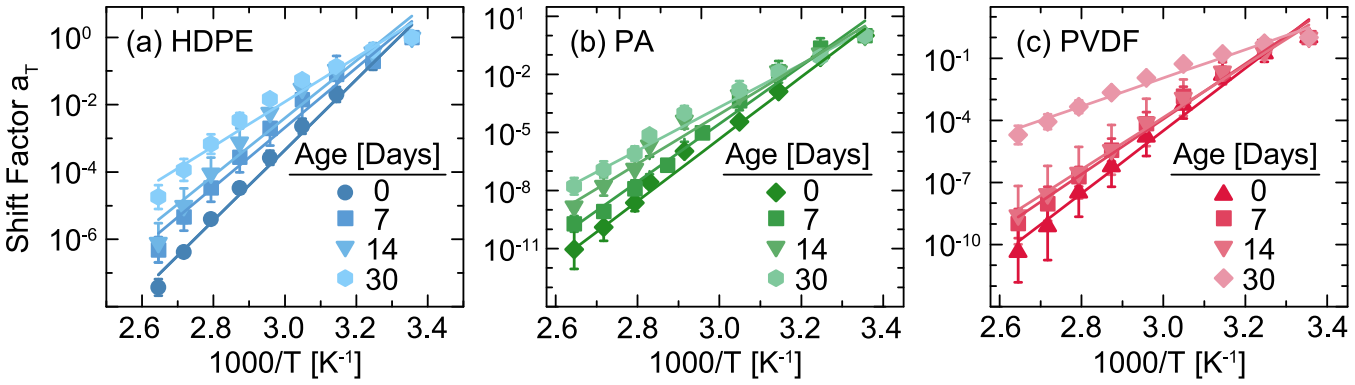


**Figure 4.** Shift factors $a_T$ for (a) HDPE, (b) PA and (c) PVDF as a function of inverse $T^{-1}$ after different aging periods. Curves are fits to eq 2. All $R^2$ values are greater than 0.95.

exhibits a more modest change up to 14 days of aging before a significant drop after 30 days of aging. These differences may be caused by differences in the levels of crystallinity, gas solubility, or the temperature of aging relative to $T_g$ or the melting temperature $T_m$. Based on reported permeability measurements, the solubility of methane in HDPE, PA and PVDF is 0.36, 0.44, and 0.35 $cm^3_{STP}/cm^3$ MPa, respectively, at 70−80 °C and 10 MPa.[46] From these values, we do not expect there to be a drastic difference in the acceleration of dynamics between polymer chemistries caused by the equilibrium absorption of natural gas within the polymers. The progressive decrease in activation energy with aging time indicates that while natural gas exposure does not significantly affect Young's modulus $E$ and the yield stress $\sigma_y$, it does substantially alter the segmental relaxation dynamics of these polymers. We believe the enhanced sensitivity of activation energy relative to these other metrics is primarily caused by the importance of time scales; the activation energy characterizes changes in viscoelastic moduli over 8 orders of magnitude in time (and correspondingly 80 °C in temperature) whereas $E$ and $\sigma_y$ are only measured over a single order in time and a single temperature of 25 °C. Thus, even subtle changes caused by gas absorption will manifest in the long-time viscoelastic relaxations without significantly altering the polymer mechanics at room temperature.

We quantify this decrease in activation energy $E_a$ as a function of aging time in Figure 5. We normalize $E_a$ by the value measured for neat samples prior to aging $E_{a,0}$ to identify relative changes, facilitating easier comparisons between polymer chemistries. As expected from the qualitative observations above, we find a monotonic decrease in $E_a$ across all polymer chemistries. After 30 days of accelerated aging, the activation energies decrease to ≈40 − 60% of their original values. Because the terminal relaxation time $\tau$ of polymers is proportional to $a_T$, this significant decrease in $E_a$ implies an acceleration of $\tau_{aged}/\tau_{neat} \approx 10^{-1}$ to $10^{-6}$. Physically, this shift in relaxation time may dramatically increase the creep failure of polymer solids,[40,47,48] in the presence of natural gas despite no detectable changes in the viscoelastic moduli. Additionally, we conducted similar aging experiments at room temperature to determine whether this observed change to polymer dynamics depends strongly on environmental conditions. Polymers aged at room temperature consistently exhibit a weaker suppression of $E_a$ than polymers aged at elevated temperatures, suggesting that the changes to $E_a$ occur more rapidly at elevated temperatures. Within the error of our measurements, however,

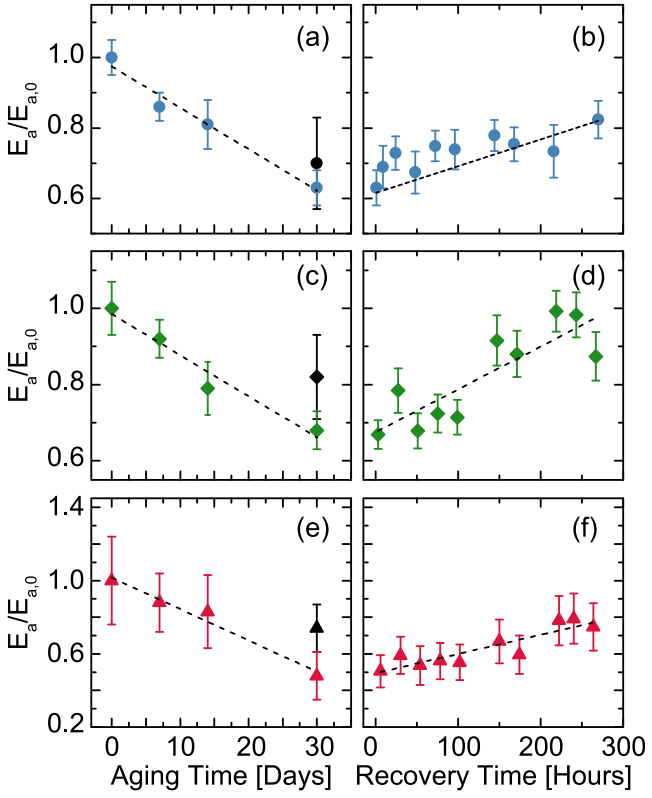


**Figure 5.** Normalized activation energy $E_a/E_{a,0}$ and the recovery tests of aged samples for (a) and (b) HDPE, (c) and (d) PA and (e) and (f) PVDF. Black symbols represent measurements taken after aging at room temperature. Dashed lines are guides to the eye.

these differences are not statistically significant. Thus, changes to polymer relaxations manifest similarly across various environmental conditions, including a range of temperatures over which these polymers would be expected to perform in pipeline applications.[5]

**3.3. Mechanisms of Gas Aging.** We hypothesize that this decrease in $E_a$ upon exposure to natural gas is driven by the absorption of small molecules within the polymer. Once absorbed, these gas molecules act as plasticizers to enhance local dynamic fluctuations. We rationalize this hypothesis through some rough estimates of the saturation time for diffusion of gas penetrants into the polymer solids. The diffusion process can be modeled through a one-dimensional Fick's law


https://doi.org/10.1021/acs.iecr.5c02255
Ind. Eng. Chem. Res. XXXX, XXX, XXX−XXX

$$\frac{\partial C}{\partial t} = D\frac{\partial^2 C}{\partial x^2} \tag{3}$$

where $C(x,t)$ is concentration at position $x$ and time $t$, and $D$ is diffusivity. With a constant external concentration $C_0$, the solution at the centerline is given by

$$C(x = 0, t) = C_0 - \frac{4C_0}{\pi}\sum_{n=0}^{\infty}\frac{1}{2n+1}\sin\left(\frac{(2n+1)\pi x}{L}\right) \exp\left(-\frac{(2n+1)^2\pi^2 Dt}{L^2}\right) \tag{4}$$

where $L$ is the thickness of the polymer sample. Using estimated values of $D = 0.41-6.5 \times 10^{-7}$ cm$^2$/s,[46] we find that the saturation time necessary for the concentration at the center to reach 95% of the concentration at the surface ranges from approximately 10 to 25 days. On longer time scales, we would therefore expect the decrease in $E_a$ to plateau as the gas reaches full saturation.

Under this physical picture, the decrease in $E_a$ should be reversible once the polymers are removed from the saturating natural gas environment. To assess their reversibility, we monitored $E_a$ after removing the samples from the pressure chambers after the 30-day aging period and stored at ambient laboratory conditions over a range of times from <1 h to >10 days before DMA testing. At ambient pressure, the primary driving force of physicochemical absorption would be removed and the aged polymers would therefore be oversaturated with gas molecules. Thus, the absorbed gas would begin to diffuse out of the polymer solids into the ambient atmosphere. We observe a gradual restoration of the $E_a$ toward the original values, as shown in Figure 5. The error bars represent the uncertainty in the linear regression of the Arrhenius plots rather than from multiple sample measurements because each complete temperature sweep required approximately 3 h of testing time, making repeated measurements impractical within the recovery time frame. This recovery phenomenon, observed for all polymer chemistries, strongly suggests that the natural gas molecules gradually diffuse out of the polymer matrices under ambient conditions. The reduction in absorbed gas correspondingly slows the fluctuation dynamics of the polymer chains and increases $E_a$. Furthermore, the reversibility of this measurement indicates that the reduction in $E_a$ is caused by *physical* changes to the polymers without inducing permanent chemical changes. Although the recovery is qualitatively similar for all polymers, there are quantitative differences with PA showing the most significant recovery after about 300 h, nearly reaching to its original activation energy. Both HDPE and PVDF recover to nearly 80% of their original activation energy, and we expect that this trend would continue toward 100% recovery over longer periods of time. These recovery measurements provide indirect evidence that the polymers absorb the natural gas molecules under elevated pressures.

To gain direct evidence that the concentration of natural gas increases in the polymer samples, we measure the Fourier Transform Infrared (FTIR) absorbance spectra of the polymer solids before and after exposure to natural gas (Figure 6). For the neat polymers, we observe spectra that are in good agreement with literature reports.[49−51] Specifically, we identify characteristic peaks at 1630 cm$^{-1}$ for PA, corresponding to the stretching of the C═O bond, and at 1178 cm$^{-1}$ for PVDF,

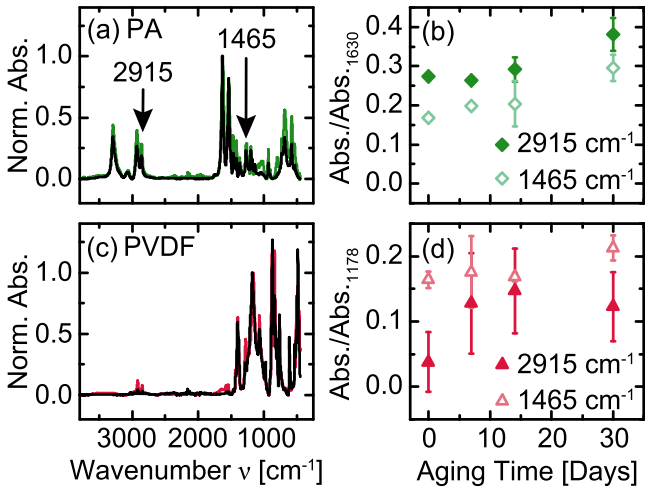


**Figure 6.** FTIR absorbance as a function of wavenumber $\nu$ normalized to peak intensity at 1630 cm$^{-1}$ corresponding to C═O stretching for (a) PA and at 1178 cm$^{-1}$ corresponding to C−F stretching for (c) PVDF. Black curves are neat samples and colored curves have been aged at 90 °C for 30 days. (b,d) Normalized absorbance of peaks at 1465 cm$^{-1}$ (open) corresponding to C−H bending and 2915 cm$^{-1}$ corresponding to C−H stretching as a function of aging time at 90 °C.

corresponding to the stretching of the C−F bond. Both of these bonds are unique to the polymer chemistries and are not found in the natural gas mixtures. Thus, they serve as a baseline against which we can compare the relative change in peak heights corresponding to bonds in the natural gas mixture. We normalize the spectra before and after exposure to the height of these peaks, respectively, and then quantify the change in the height of peaks at $\nu$ = 2915 and 1465 cm$^{-1}$, which correspond to the bending and stretching of the alkane C−H bond, respectively. Quantitatively, we observe an increase in the relative height of these peaks for both PA and PVDF as a function of exposure time, indicating that there is an increase in the density of C−H bonds within the solids. We do collect spectra for comparable measurements on the HDPE samples (Supporting Information), but because HDPE does not possess a unique bond chemistry with which to evaluate changes in natural gas content, we are unable to quantify gas absorption. Nevertheless, these FTIR results demonstrate that the polymers absorb natural gas molecules under elevated pressures, confirming our hypothesized mechanism underlying the changes to $E_a$, in which the natural gas penetrates the polymers and acts as a plasticizer to accelerate relaxation dynamics. Moreover, the FTIR results do not reveal the development of new peaks, indicating that there are no significant chemical reactions occurring between the polymer and natural gas environment during our aging protocol. This lack of chemical changes is further supported by DSC and XRD measurements (Figures S4 and S5, respectively), which show no significant changes in phase transitions and crystallinity with respect to gas aging.

## 4. CONCLUSION

Polymeric liners serve as a cost-effective option to remediate aging natural gas pipelines, but their performance over extended operational lifetimes is still unknown. By aging representative polymers in the presence of a model natural gas environment at an elevated temperature and pressure, we have


https://doi.org/10.1021/acs.iecr.5c02255
Ind. Eng. Chem. Res. XXXX, XXX, XXX−XXX

demonstrated that the polymers maintain their mechanical integrity; neither elastic modulus nor yield stress, two key mechanical properties of solids, show any significant change as a function of exposure to natural gas environments. We notice, however, that the viscoelastic dynamics exhibit a strong dependence on exposure to natural gas. The activation energy $E_a$ of the solids decreases by up to 50%, representing a dramatic acceleration of segmental dynamics within the melt. We rationalize this change through a physical mechanism by which the solids absorb small gas molecules that act as plasticizers. To confirm this hypothesis, we have shown that there is an increase of natural gas molecules within the solids after exposure and that upon removal of the polymers into ambient conditions, $E_a$ recovers to nearly its original values. Together, these findings suggest that polymer liners can serve as a safe and effective option for remediating gas pipelines, especially under lower operating pressures. The accelerated dynamics, however, may result in changes to the creep response of these materials under prolonged operation. Furthermore, we caution that such reversibility may be unique to the natural gas composition chosen for this study, which contains pure alkanes that are chemically stable and have low reactivity. Real-world natural gas compositions may contain more reactive species such as $H_2S$, $O_2$, $H_2O$, or reactive organic species that may chemically interact with specific polymers to drive irreversible changes to the mechanical and dynamical properties of the solids. We plan to assess the impacts of these contaminants on polymer properties in future work.

## ■ ASSOCIATED CONTENT

### Supporting Information

The Supporting Information is available free of charge at https://pubs.acs.org/doi/10.1021/acs.iecr.5c02255.

Tensile testing data for all three polymers, differential scanning calorimetry (DSC) thermograms showing thermal transitions, X-ray diffraction (XRD) patterns characterizing crystallinity changes, and FTIR spectra for HDPE samples before and after aging (PDF)

## ■ AUTHOR INFORMATION


### Corresponding Author

**Ryan Poling-Skutvik** − *Department of Chemical, Biomolecular, and Materials Engineering, University of Rhode Island, Kingston, Rhode Island 02881, United States; Department of Physics, University of Rhode Island, Kingston, Rhode Island 02881, United States;* orcid.org/0000-0002-1614-1647; Email: ryanps@uri.edu

### Authors

**Mohammadjavad Haji Rezaei** − *Department of Chemical, Biomolecular, and Materials Engineering, University of Rhode Island, Kingston, Rhode Island 02881, United States*

**Aiden Ferreira** − *Department of Chemical, Biomolecular, and Materials Engineering, University of Rhode Island, Kingston, Rhode Island 02881, United States*

**Maile Campbell** − *Department of Chemical, Biomolecular, and Materials Engineering, University of Rhode Island, Kingston, Rhode Island 02881, United States*

**Deepro Ghosh** − *School of Engineering, Brown University, Providence, Rhode Island 02912, United States;* orcid.org/0009-0004-9492-2774

**Keven Alkhoury** − *School of Engineering, Brown University, Providence, Rhode Island 02912, United States;* orcid.org/0000-0002-1244-3226

**Zakhar Lyakhovych** − *School of Engineering, Brown University, Providence, Rhode Island 02912, United States*

**Edith Mathiowitz** − *School of Engineering, Brown University, Providence, Rhode Island 02912, United States; Department of Pathology and Laboratory Medicine, Brown University, Providence, Rhode Island 02912, United States;* orcid.org/0000-0003-3054-7130

**Vikas Srivastava** − *School of Engineering, Brown University, Providence, Rhode Island 02912, United States; Institute for Biology, Engineering, and Medicine, Brown University, Providence, Rhode Island 02912, United States;* orcid.org/0000-0001-5480-2349

Complete contact information is available at: https://pubs.acs.org/10.1021/acs.iecr.5c02255


### Notes

The authors declare no competing financial interest.

## ■ ACKNOWLEDGMENTS

This work was supported by the United States Department of Transportation Grant 693JK32250001CAAP. The views and opinions expressed in this article are those of the authors and do not necessarily reflect the official policy or position of any agency of the U.S. government.

## ■ REFERENCES


(1) *Department of Transportation, Pipeline Mileage and Facilities.* https://www.phmsa.dot.gov/data-and-statistics/pipeline/pipeline-mileage-and-facilities,2023.

(2) Kass, M. D.; Keiser, J. R.; Liu, Y.; Moore, A.; Polsky, Y. Assessing Compatibility of Natural Gas Pipeline Materials with Hydrogen,CO2, and Ammonia. *J. Pipeline Syst. Eng. Pract.* **2023**, *14*, 04023007.

(3) *Department of Transportation, Pipeline Replacement Background.* https://www.phmsa.dot.gov/data-and-statistics/pipeline-replacement/pipeline-replacement-background,2025.

(4) Saji, V. S. *Corrosion Inhibitors in the Oiland Gas Industry*; John Wiley & Sons: Incorporated: Newark, 2020.

(5) Khalid, H. U.; Ismail, M. C.; Nosbi, N. Permeation Damage of Polymer Liner in Oil and Gas Pipelines: A Review. *Polymers* **2020**, *12*, 2307.

(6) Iannuzzi, M.; Barnoush, A.; Johnsen, R. Materials and Corrosion Trends in Offshore and Subsea Oil and Gas Production. *NPJ. Mater. Degrad.* **2017**, *1*, 2.

(7) Wang, Y.; Lan, H.-Q.; Meng, T. Lifetime Prediction of Natural Gas Polyethylene Pipes with Internal Pressures. *Eng. Fail. Anal.* **2019**, *95*, 154−163.

(8) Strube, J.; Thiede, B. C.; Auch, W. E. Proposed Pipelines and Environmental Justice: Exploring the Association between Race, Socioeconomic Status, and Pipeline Proposals in the United States*. *Rural Sociol.* **2021**, *86*, 647−672.

(9) Matthews, J. C.; Allouche, E. N.; Sterling, R. L. Social Cost Impact Assessment of Pipeline Infrastructure Projects. *Environ. Impact Assess. Rev.* **2015**, *50*, 196−202.

(10) Xi, D.; Lu, H.; Zou, X.; Fu, Y.; Ni, H.; Li, B. Development of Trenchless Rehabilitation for Underground Pipelines from an Academic Perspective. *Tunn. Undergr. Space Technol.* **2024**, *144*, 105515.

(11) Kaushal, V.; Najafi, M.; Serajiantehrani, R. Environmental Impacts of Conventional Open-Cut Pipeline Installation and Trenchless Technology Methods: State-of-the-Art Review. *J. Pipeline Syst. Eng. Pract.* **2020**, *11*, 03120001.

(12) Jung, Y. J.; Sinha, S. K. Evaluation of Trenchless Technology Methods for Municipal Infrastructure System. *J. Infrastruct. Syst.* **2007**, *13*, 144−156.
(13) Rueda, F.; Otegui, J. L.; Frontini, P. Numerical Tool to Model Collapse of Polymeric Liners in Pipelines. *Eng. Failure Anal.* **2012**, *20*, 25−34.
(14) Esaklul, K. A.; Mason, J. *Trends in Oil and Gas Corrosion Research and Technologies*; Woodhead Publishing, 2017; pp 627−660.
(15) Khelif, R.; Chateauneuf, A. Reliability-Based Replacement of Polyethylene Gas Pipeline Networks. *Arab. J. Sci. Eng.* **2014**, *39*, 8175−8185.
(16) Karim, M. A.; Abdullah, M. Z.; Deifalla, A. F.; Azab, M.; Waqar, A. An Assessment of the Processing Parameters and Application of Fibre-Reinforced Polymers (FRPs) in the Petroleum and Natural Gas Industries: A Review. *Results Eng.* **2023**, *18*, 101091.
(17) Gogolinskiy, K. V.; Vinogradova, A. A.; Kopylova, T. N.; Povarov, V. G.; Vasilev, E. A.; Shchiptsova, E. K.; Rybkin, D. E.; Kolobov, D. S. Study of Physicochemical Properties of Polyethylene Gas Pipelines Material with a Prolonged Service Life. *Int. J. Press Vessel Pip* **2022**, *200*, 104825.
(18) Arjun, M.; Kaushal, V.; Shirkhanloo, S.; Rahman, S.; Najafi, M. *A Review of Rehabilitation Methods for Aging Pipe Culverts by Spray AppliedPipe Lining, Grouting, and Sliplining*; Pipelines, 2023, 252−259.
(19) Ji, H. W.; Koo, D. D.; Kang, J.-H. Short- and Long-Term Structural Characterization of Cured-in-Place Pipe Liner with Reinforced Glass Fiber Material. *Int. J. Environ. Res. Public Health* **2020**, *17*, 2073.
(20) Syachrani, S.; Jeong, H. S. D.; Rai, V.; Chae, M. J.; Iseley, T. A Risk Management Approach to Safety Assessment of Trenchless Technologies for Culvert Rehabilitation. *Tunn. Undergr. Space Technol.* **2010**, *25*, 681−688.
(21) Reyna, S. M.; Vanegas, J. A.; Khan, A. H. Construction Technologies for Sewer Rehabilitation. *J. Constr Eng. Manage.* **1994**, *120* (3), 467−487.
(22) Sanders, E. Penetrant-Induced Plasticization and Gas Permeation in Glassy Polymers. *J. Membr. Sci.* **1988**, *37*, 63−80.
(23) Semenova, S. I.; Ohya, H.; Smirnov, S. I. Physical Transitions in Polymers Plasticized by Interacting Penetrant. *J. Membr. Sci.* **1997**, *136*, 1−11.
(24) Minelli, M.; Sarti, G. C. Permeability and Diffusivity of CO2 in Glassy Polymers with and without Plasticization. *J. Membr. Sci.* **2013**, *435*, 176−185.
(25) Swaidan, R.; Ghanem, B.; Litwiller, E.; Pinnau, I. Physical Aging, Plasticization and Their Effects on Gas Permeation in"Rigid" Polymers of Intrinsic Microporosity. *Macromolecules* **2015**, *48*, 6553−6561.
(26) Pandey, P.; Chauhan, R. S.; Shrivastava, A. K. Carbon-dioxide-induced Plasticization Effects in Solvent-cast Polyethylene Membranes. *J. Appl. Polym. Sci.* **2002**, *83*, 2727−2731.
(27) Baatti, A.; Erchiqui, F.; Godard, F.; Bussieres, D.; Bebin, P. DMA Analysis, Thermal Study and Morphology of Polymethylsilsesquioxane Nanoparticles-Reinforced HDPE Nanocomposite. *J. Therm. Anal. Calorim.* **2020**, *139*, 789−797.
(28) Zeltmann, S. E.; Bharath Kumar, B.; Doddamani, M.; Gupta, N. Prediction of Strain Rate Sensitivity of High Density Polyethylene Using Integral Transformof Dynamic Mechanical Analysis Data. *Polymer* **2016**, *101*, 1−6.
(29) Mano, J.; Sencadas, V.; Costa, A.; Lanceros Mendez, S. Dynamic Mechanical Analysis and Creep Behaviour of $\beta$-PVDF Films. *Mater. Sci. Eng* **2004**, *370*, 336−340.
(30) Sencadas, V.; Barbosa, R.; Mano, J. F.; Lanceros Mendez, S. Mechanical Characterization and Influence of the High Temperature Shrinkageof $\beta$-PVDF Films on Its Electromechanical Properties. *Ferroelectrics* **2003**, *294*, 61−71.
(31) Simoes, R. D.; Job, A. E.; Chinaglia, D. L.; Zucolotto, V.; Camargo Filho, J. C.; Alves, N.; Giacometti, J. A.; Oliveira, O. N.; Constantino, C. J. L. Structural Characterization of Blends Containing Both PVDF and Natural Rubber Latex. *J. Raman Spectrosc.* **2005**, *36*, 1118−1124.
(32) Gnatowski, A.; Koszkul, J. Investigation on PA/PP Mixture Properties by Means of DMTA Method. *J. Mater. Process. Technol.* **2006**, *175*, 212−217.
(33) Kehrer, L.; Keursten, J.; Hirschberg, V.; Bohlke, T. Dynamic Mechanical Analysis of PA 6 under Hydrothermal Influences and Viscoelastic Material Modeling. *J. Thermoplast. Compos. Mater.* **2023**, *36*, 4630−4664.
(34) Folga, S. *Natural Gas Pipeline Technology Overview*; OSTI.GOV 2007.
(35) Mohammadi, M.; Yousefi, A. A.; Ehsani, M. Thermorheological Analysis of Blendof High- and Low-Density Polyethylenes. *J. Polym. Res.* **2012**, *19*, 9798.
(36) Shangguan, Y.; Chen, F.; Jia, E.; Lin, Y.; Hu, J.; Zheng, Q. New Insight into Time-Temperature Correlation for Polymer Relaxations Ranging from Secondary Relaxationto Terminal Flow: Application of a Universal and Developed WLF Equation. *Polymers* **2017**, *9*, 567.
(37) Sencadas, V.; Lanceros Mendez, S.; Sabater ISerra, R.; Andrio Balado, A.; Gomez Ribelles, J. L. Relaxation Dynamics ofPoly-(Vinylidene Fluoride) Studied by Dynamical Mechanical Measurements and Dielectric Spectroscopy. *Eur. Phys. J. E* **2012**, *35*, 41.
(38) Ariza Gomez, A. J.; Contreras, M. M.; Vaz, M. A.; Costa, C. A.; Costa, M. F. Temperature-Time Large Strain Mechanical Model for Poly(VinylideneFluoride). *Polym. Test.* **2020**, *82*, 106312.
(39) Luo, W.; Wang, C.; Hu, X.; Yang, T. Long-Term Creep Assessment of Viscoelastic Polymer by Time-Temperature-Stress Superposition. *Acta Mech Sol Sin.* **2012**, *25*, 571−578.
(40) Lai, J.; Bakker, A. Analysis of the Non-Linear Creep of High-Density Polyethylene. *Polymer* **1995**, *36*, 93−99.
(41) Zhao, Y.; Lu, Z.; Yao, H.; Hu, H.; Li, X.; Tang, Y. A Fast and Precise Methodology of Creep Master Curve Construction for Geosynthetics Based on Stepped Isothermal Method (SIM). *Geotext Geomembr.* **2021**, *49*, 952−962.
(42) Rubinstein, M.; Colby, R. H. *Polymer Physics*; Oxford University Press: New York, 2003.
(43) Mano, J.; Sousa, R.; Reis, R.; Cunha, A.; Bevis, M. Viscoelastic Behaviour and Time−Temperature Correspondence of HDPE with Varying Levels of Process-Induced Orientation. *Polymer* **2001**, *42*, 6187−6198.
(44) Boucenna, Y.; Layachi, A.; Cherfia, A.; Laoutid, F.; Satha, H. Non-Isothermal Crystallization Kinetics and Activation Energy for Crystal Growth of Polyamide 66/Short Glass Fiber/Carbon Black Composites. *Materials* **2023**, *16*, 7073.
(45) Silva, A. J. D. J.; Nascimento, C. R.; Da Costa, M. F. Thermomechanical Properties and Long-Term Behavior Evaluation of Poly(Vinylidene Fluoride)(PVDF) Exposed to Bioethanol Fuel under Heating. *J. Mater. Sci.* **2016**, *51*, 9074−9094.
(46) Flaconneche, B.; Martin, J.; Klopffer, M. H. Permeability Diffusion and Solubility of Gases in Polyethylene, Polyamide 11 and Poly (Vinylidene Fluoride). *OGST* **2001**, *56*, 261−278.
(47) Yang, J.-L.; Zhang, Z.; Schlarb, A. K.; Friedrich, K. On the Characterization of Tensile Creep Resistance of Polyamide 66 Nanocomposites. Part II: Modeling and Prediction of Long-Term Performance. *Polymer* **2006**, *47*, 6745−6758.
(48) Kraft, M.; Meissner, J.; Kaschta, J. Linear Viscoelastic Characterization of Polymer Melts with Long Relaxation Times. *Macromolecules* **1999**, *32*, 751−757.
(49) Smith, B. C. The Infrared Spectra of Polymers II: Polyethylene. *Spectroscopy* **2021**, *24*, 29.
(50) Cheval, N.; Gindy, N.; Flowkes, C.; Fahmi, A. Polyamide 66 Microspheres Metallised with in Situ Synthesised Gold Nanoparticles for a Catalytic Application. *Nanoscale Res. Lett.* **2012**, *7*, 182.
(51) Cai, X.; Lei, T.; Sun, D.; Lin, L. A Critical Analysis of the $\alpha$, $\beta$ and $\gamma$ Phases in Poly(Vinylidene Fluoride) Using FTIR. *RSC Adv.* **2017**, *7*, 15382−15389.


https://doi.org/10.1021/acs.iecr.5c02255
Ind. Eng. Chem. Res. XXXX, XXX, XXX−XXX